Characterization of zebra mussel transport near a pump intake

R. A. Tatara
Northern Illinois University
tatara@ceet.niu.edu

D. R. Poe
CSI Technologies, Inc.
dpoe@csitechnologies.com

G. M. Lupia
CSI Technologies, Inc.
greg.lupia@exeloncorp.com

ABSTRACT

The appearance and explosive population growth of zebra mussels have impacted many facilities near water, such as electricity-generating power plants. These mussels can congregate at plant-water-intake structures where proactive maintenance actions, such as mussel kills, must be performed. However, once dead, the mussel debris is a potential contaminant drawn into the plant via cooling water pump suctions; this may affect piping and components downstream of the pump suctions. Thus, it becomes necessary to establish whether sufficient water velocity, from the suction action of a pump, exists to entrain shell debris. Although entrainment data for zebra mussel shells and shell fragments are lacking, this study employs a generalized empirical method based on other types of bivalve shells. Basic pump-suction considerations yield an entrainment volumetric zone in which any shells would be drawn into the pump. A calculated sample zone extends slightly less than one meter from the centerline of the pump-suction pipe and is cylindrical in shape. This approach can be generalized to various pump intake configurations and bivalves, providing a predictive means for evaluating plant system contaminants. Experimental data, although outside the scope of this study, may be used to refine the modeling.

INDEX TERMS

Pump intakes, Sedimentation, Shell entrainment, Zebra mussels

I. INTRODUCTION

The infiltration and dramatic population growth of zebra mussels (*Dreissena polymorpha*) have impacted many facilities near water. Electricity-generating power plants are just one example of affected facilities. The mussels can congregate at plant-water-intake structures where the water environment is favorable to the organism, with plant inspections detecting large, sharp increases in the concentration of the mussels. To avoid potential clogging of intake-structure components, corrective actions are called for, including a mussel kill. However, as the kill proceeds, the mussels detach, resulting in relic mussel shells and mats of mussel shells in the water, which may be drawn into a power plant through its intake-cooling water pumps.

Cooling water pumps typically are of the vertical-centrifugal type and draw water from the intake structure. Along with drawing water into the suction of each pump, there is the potential to entrain any debris, including biogenic such as relic zebra mussel shells. The amount of entrainment, if any, is determined by a variety of factors such as pump performance, suction location, debris location, and debris concentration. Any analysis must consider the flow field radiating from the pump-suction region as well as the entrainment characteristics of the shells.

Furthermore, to potentially assess the impact of shell debris upon components (heat exchangers, filters, strainers, valves, instrumentation, etc.) inside the plant, it becomes necessary to determine the number of zebra mussels transported through the intake pumps. This depends upon the concentration and location of mussel deposits.

II. ENTRAINMENT OF DEBRIS

Velocity along the bottom and throughout the intake structure provides the driving force for sediment transport where the sediment, in this case,

would be the biogenic debris of dead zebra mussels (relic shells). The debris from one organism would be soft tissue and two half-shells could detach. Assuming any soft tissues passing completely through the cooling system, it is the shells that have the potential of clogging components downstream of the pumps. Although local velocities under 0.3 m/sec are thought to settle out most common debris [1], mussel half-shells are more prone to entrainment than sand and gravel.

The hydrodynamics of sedimentation transport are complex. As water flows over a collection of loose particles, hydrodynamic forces are generated and act upon the particles (grains). The forces involve lift, frictional drag, and turbulence. Within the grains there is a distribution of different sizes and shapes affecting these forces. One parameter of importance is the critical condition when the grain moves. An assumption can be made that if sufficient flow-shear forces exist to move the grain, it will be completely entrained or it will creep towards a pump suction (increasing-velocity field). In both cases, the grain eventually enters the pump. This situation exists no matter the types of loose grains present.

Early entrainment studies defined a critical or competent velocity as the bulk fluid velocity at the bed (bottom) of the channel that initiated grain movement. An early correlation was developed by Mavis, Ho, and Tu [2]:

$$(U_b)_{cr} = 0.5 \cdot d^{4/9} \cdot \left(\frac{\rho_s}{\rho} - 1 \right)^{1/2} \qquad (1)$$

where $(U_b)_{cr}$ = critical bottom velocity, ft/sec; d = mean grain diameter, mm; ρ_s = grain density; and ρ = water density. This correlation used several different sand and rock grains ranging in size from 0.35 mm to 5.7 mm having a specific density (ρ_s / ρ) of 1.83 or 2.64. More modern research led to the use of the Shields diagram, where the same entrainment-initiation velocity is expressed in terms of shear stress. The diagram correlates many entrainment studies using a variety of grains including sand, glass, and steel shot. The critical velocity can be directly calculated from the shear-stress parameter. However, it should be noted that applying the Shields diagram to irregularly shaped grains, particularly those of mussel shells, would result in a very large uncertainty in values. In fact, studies on settling velocities and entrainment of shell fragments demonstrated large divergence between measured results and Shields diagram predictions; it is apparent the shell material behaves much differently from typical sediment, even when particle sizes and densities are the same [3].

Collins and Rigler [4] found an improvement over the standard Shields diagram by using the settling velocity, w_s, which better accounts for irregularity in grain shape. They defined a Movability number, the ratio of the critical velocity to the settling velocity as well as a correlation for critical bottom velocity (cm/s):

$$(U_b)_{cr} = \left(\frac{1.24}{\rho} w_s^{0.33} \right)^{1/2} \quad \text{for } w_s < 10 \text{ cm/s} \qquad (2)$$

where ρ = water density in g/cm3. Extending this approach directly to shell data, Paphitis [3] studied two different density shell fragments, 2.72 and 2.80 specific gravity, ranging in size from 0.28 mm to 0.90 mm as measured via a sieve diameter; it was found the Movability number plotted against a grain Reynolds number better correlated the motion of irregularly shaped shell pieces. This represents an improved calculation methodology for irregular shapes such as bivalve shells.

Certainly any shell fragment data correlates better with the Movability number. However, the Movability-based method does require knowledge or calculation of a settling velocity. A more accurate modeling should involve the use of actual biogenic-bivalve data; such data are scarce in the literature, but two studies are available. First, Kelling and Williams [5] tested the interaction of pebbles or one type of mussel shell (Mytilus edulis) and water flow. This study was only interested in the reorientation of the shell subject to the channel flow field; full entrainment did not take place. Second, there exists an extensive source of bivalve data by Allen [6], which looked at 16 different shell types. The resulting data included settling (terminal-fall) velocities, drag coefficients, and critical-entrainment velocities for shell concave-up and convex-up orientations. A dimensionless entrainment factor is presented as:

$$\Theta = \frac{\rho \cdot (U_m)_{cr}^2}{(M/A) \cdot \left(\frac{\sigma - \rho}{\sigma}\right) \cdot g} \quad (3)$$

where Θ = dimensionless fluid force or entrainment factor available for each bivalve, ρ = water density, U_m = mean fluid velocity required to entrain shell, M = dry mass of shell, A = maximum-shell-projected area, σ = shell density, and g = acceleration due to gravity. This likely represents the most accurate prediction of shell entrainment velocity if the shell in question is reasonably close to one of the 16 available in this study.

III. ENTRAINMENT OF ZEBRA MUSSEL DEBRIS

Drawing from Allen [6] to compute an entrainment velocity for the zebra mussel, typical zebra mussel data were matched to the dimensions of one of the 16 bivalves. Based on a general understanding of the size, shape, and shell texture of a zebra mussel, it was determined that it most closely matches the bivalve *Mytilus edulis*. Size and density ranges for the zebra mussel species were considered; for conservatism in the modeling, the lowest values in the range are used, as these would require the least velocity to entrain. Table I, in conjunction with Figure 1, lists the typical mussel dimensions used for the present analysis.

Table I. Mussel shell data [6]

Dimension	Description	Value
a	Length	2.03×10^{-2} m
b	Height	1.18×10^{-2} m
c	Thickness	0.35×10^{-2} m
M	Dry Mass	0.253×10^{-3} kg
σ	Solid Density	2510 kg/m^3
$A = a \cdot b$	Maximum-Shell-Projected Area	2.40×10^{-4} m^2

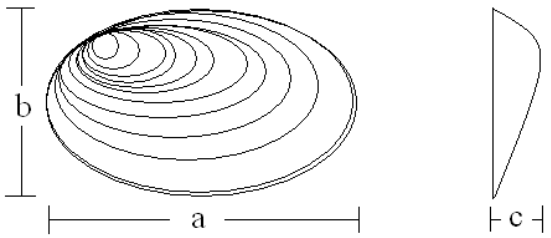

Figure 1. Main dimensions of an idealized bivalve shell

Using the physical data, the dimensionless entrainment factor was found and the minimum velocity required to entrain a mussel shell was calculated using (3):

$$U_m = \sqrt{\frac{\Theta \cdot M \cdot (\sigma - \rho) \cdot g}{A \cdot \rho \cdot \sigma}} \quad (4)$$

The entrainment factor, Θ, is a function of the Reynolds number calculated in (5), for each bivalve:

$$\mathrm{Re} = \frac{DV\rho}{\mu} = \frac{VD}{\upsilon} \quad (5)$$

where D = equivalent shell diameter, V = terminal-fall velocity of shell, ρ = bulk-water density, μ = water dynamic viscosity, and υ = water kinematic viscosity. The equivalent shell diameter is determined from the projected area of the shell as follows:

$$D = \sqrt{\frac{4A}{\pi}} \quad (6)$$

The terminal-fall velocity is correlated with the unit immersed mass *UIM* (immersed mass per unit projected area) which is set by equation [6]:

$$UIM = \frac{M(\sigma - \rho)}{A\sigma} \quad (7)$$

where M = dry mass of shell, A = maximum-shell-projected area, σ = shell density, ρ = water density, and finally, terminal-fall velocity is correlated by:

$$V = 0.134\ (UIM)^{1/2} \quad (8)$$

IV. PUMP-SUCTION FLOW FIELD

Centrifugal pumps have a rotating impeller within a casing. As the impeller rotates, the blade action locally reduces the pressure, which pulls water to the impeller through the suction piping. The influence of this suction extends past the suction-pipe entrance bell and into the surrounding body of water. The extent of influence depends on the power of the pump, the suction piping geometry, and the intake or intake pit geometry. For proper pump op-

eration, ensure the approach velocity to the suction of the pump is uniform and without rotation from vortexes or swirling. Baffling, turning vanes, and suction cones are installed to better direct the incoming water.

Regardless of the velocities, enough space must be allowed around the suction bell to draw the rated capacity of the pump. Guidelines are available dictating the four important installation specifications: the typical suction bell-to-bottom clearance, the minimum width clearance, the typical wall-to-bell distance, and the normal water level which dictates the suction inlet submergence [1]. The guidelines are based on the rated pump flow capacity. For modeling purposes, the dimensions needed to ensure adequate suction flow can be thought of as forming a type of volume of influence; perhaps hemispherical, cylindrical, irregular cylindrical, or any other assumed volume. The suction influence is strongest within this volume and decreases further away from the suction bell. Directly below the suction bell and extending down to the intake floor, the bell exerts the strongest suction (lifting) and highest local velocities. In other areas extending out radially from the centerline of the pump, the suction action is greatly reduced with a corresponding decrease in local velocities. The local pressure as measured in the intake water is also decreasing, but the actual values are not of interest. However, it should be remembered that it is the pressure difference from the intake water to impeller suction that provides the driving force for the flow (velocities). Once some volume of influence is defined, the average velocities entering this space may be computed.

Under steady-state conditions all the water (fluid) entering the outer perimeter area of any volume of influence must pass through the volume and exit (enter the suction bell). In such a case, the continuity equation may be applied as:

$$\int_{cs} \rho \hat{n} \cdot V dA = 0 \qquad (9)$$

where ρ = fluid density, $\hat{n}$ = unit normal vector, V = velocity vector, and A = area across which fluid enters/exits the control volume. Assuming uniform flow with one inlet (the outer-volume-perimeter area) and one exit (the suction bell), the equation reduces to: $\rho_i A_i V_i - \rho_s A_s V_s = 0$ and $\rho_s A_s V_s = \rho_i A_i V_i = \dot{m}_p$ where the subscripts s and i refer to suction and influence perimeter, respectively, and $\dot{m}_p$ is the mass flow rate. Assuming an isothermal and incompressible flow condition prevails, then $\rho_s = \rho_i$. The total pump volumetric flow rate (Q_p) is related to the outer-perimeter area of influence through:

$$A_i V_i = Q_p \qquad (10)$$

With (10), an average, uniform velocity can be calculated at the perimeter boundary of any defined volume of influence at any volumetric flow rate.

For the present study, the area of influence perimeter is assumed to be cylindrical, with a top disk open to water and a bottom disk bound by the pump pit floor. Additionally, the cross-sectional area of the pump-suction pipe through the top disk reduces this area. Figure 2 shows the area of influence where H is the normal water level, B is the typical suction bell-to-bottom clearance, C is the height above the bottom of the suction bell and is assumed to equal the suction bell-to-bottom clearance, and r is the pump-suction pipe radius. In conjunction with Figure 2, the following equation is used to calculate the outer area of influence for the pump:

$$A_i = 2\pi RB + \pi R^2 + 2\pi RC - \pi r^2 \qquad (11)$$

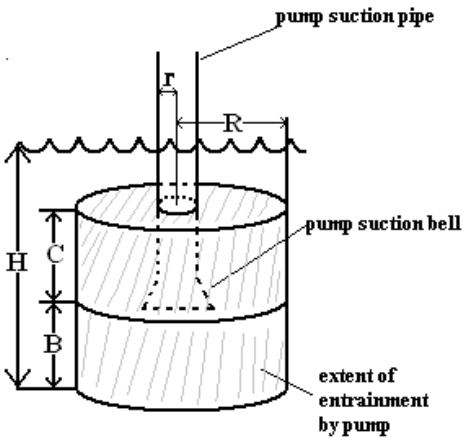

Figure 2. Pump-suction area of influence diagram

To link shell entrainment with the pump suction in Figure 2, the radius R represents the radius where the local velocity equals the computed-entrainment value or $U_m = V_i$. Thus, a volumetric zone is established within which local velocities are sufficient to entrain any shells. With this methodology,

the velocity distribution starting at the impeller suction can be computed anywhere in an intake structure. The two main assumptions of this modeling are the shape of the volume of influence and the fact that (10) yields only an average, uniform velocity at a particular distance from the intake bell. Of course, the volume and its shape can be adjusted based on the specific orientation of the pump and the intake, including taking into account obstructions, walls, and all other irregularities. (It is also possible that the pump suction will be sufficient to entrain shells beyond the intake structure and into the main channel or other regions.) Once the velocity distribution inside the cylinder is established, the next step is to model the effects of the velocity field on the mussel debris. The velocity from the pump suction is sufficient to entrain shell particles out to a critical radius, *R*, where the velocity due to pump suction drops below the entrainment velocity (U_m) calculated by (4). With this, and using an assumed or a measured-mussel-concentration distribution, the number entrained can be found, since the local velocity is known at every point away from the pump.

V. SAMPLE CALCULATION

From the zebra mussel data of Table I, the equivalent shell diameter is:

$$= \quad D = \sqrt{\frac{4(2.4x10^{-4}m^2)}{\pi}} \quad 0.0175 \text{ m} \qquad (6)$$

and the unit immersed mass is:

$$UIM = \frac{0.253x10^{-3}kg(2510-1000)kg/m^3}{2.4x10^{-4}m^2(2510kg/m^3)} = 0.634 \text{ kg/m}^2 \quad (7)$$

based on a bulk-water density of 1000 kg/m^3. Then the terminal-fall velocity of each shell is: $V = 0.134 (0.634)^{1/2} = 0.107$ m/s by (8). The Reynolds number is:

$$\text{Re} = \frac{0.107m/s(0.0175m)}{1.004x10^{-6}m^2/s} \quad = 1{,}865 \qquad (5)$$

where the kinematic water viscosity of the bulk-intake water is 1.004x10^{-6} m^2/s. Using the Reynolds number, an entrainment factor of about 3 is obtained from the graphical data of Allen [6], assuming the zebra mussel matches most closely to *Mytilus edulis*. Thus the minimum entrainment velocity is found as:

$$U_m = \sqrt{\frac{3 \cdot 0.253x10^{-3}kg(2510-1000)kg/m^3 \cdot 9.8m/}{2.4x10^{-4}m^2 \cdot 1000kg/m^3 \cdot 2510kg/m^3}} = 0.14 \text{ m/s} \quad (4)$$

Therefore, any mussel debris subject to 0.14 m/s or greater local velocity will be entrained by the pump. For a sample pump installation, $B = 0.356$ m, $C = 0.356$ m, $r = 0.305$ m, and $Q_p = 0.946$ m^3/s so that $A_i = (0.946 \text{ m}^3/\text{s}) / (0.14 \text{ m/s}) = 6.76$ m^2 by (10).

Here U_m has been substituted for V_i in the continuity equation, and *R* is easily found to be 0.95 m from (11). Any mussel shell fragments within a cylindrical volume having a radius of 0.95 m from the pump suction are assumed to be drawn into it.

Although the proposed methodology contains significant assumptions, it nevertheless is a good approach to establishing bounds for a complex problem where quantitative data and methods are lacking. Certainly, more complex refinements could be undertaken including the use of finite element modeling and other computerized analyses. Additionally, this empirically-derived approach can be extended to various pump-intake configurations and bivalves. Although outside the scope of this study, once experimental data become available, these may be helpful in refining the modeling.

VI. REFERENCES

[1] I. J. Karassik, et al., Pump Handbook, 2nd Edition. New York, NY: McGraw-Hill Book Company, Section 10.1, 1986.

[2] F. T. Mavis, C. Ho, and Y-C. Tu, "The transport of detritus by flowing water – I," *University of Iowa Studies in Engineering*, vol. 294, pp. 1-53, 1935.

[3] D. Paphitis, M. B. Collins, L. A. Nash, and S. Wallbridge, "Settling velocities and entrainment thresholds of biogenic sands (shell fragments) under unidirectional flow," *Sedimentology*, vol. 49, pp. 211-225, 2002.

[4] M. B. Collins and J. K. Rigler, "The use of settling velocity in defining the initiation of motion of heavy mineral grains, under uni-

directional flow," *Sedimentology*, vol. 29, pp. 419 – 426, 1982.
[5] G. Kelling and P. F. Williams, "Flume studies of the reorientation of pebbles and shells," *The Journal of Geology*, vol. 75, pp. 243 – 267, 1967.
[6] J. R. L. Allen, "Experiments on the settling, overturning, and entrainment of bivalve shells and related models," *Sedimentology*, vol. 31, pp. 227-250, 1984.

ROBERT A. TATARA, PhD holds a doctorate in chemical engineering from Northwestern University and has over twenty years experience in heat exchangers and cooling water systems. He is an associate professor with the Department of Technology, Northern Illinois University, DeKalb, IL 60115 USA (phone: 815-753-1130; FAX: 815-753-3702).

DANIEL R. POE is active in engineering program support for a variety of power plant issues. He is manager of new product development for CSI Technologies, Inc., East Dundee, IL 60118 USA.

GREGORY M. LUPIA was a senior technical specialist at CSI Technologies, Inc. concentrating in raw-water cooling systems analysis as well as general corrosion issues for power plants. He holds a BSME from the Illinois Institute of Technology and currently is a senior engineer specializing in cooling water systems and buried pipe corrosion with Exelon Generation Company, LLC., Warrenville, IL 60555 USA.
.